

# Lattice Radial Quantization: 3D Ising

R. C. Brower<sup>a</sup>, G. T. Fleming<sup>b</sup>, H. Neuberger<sup>c</sup> \*

<sup>a</sup> *Department of Physics, Boston University*  
*Boston, Massachusetts 02215, USA*  
`brower@bu.edu`

<sup>b</sup> *Department of Physics, Sloane Laboratory, Yale University*  
*New Haven, Connecticut 06520, USA*  
`George.Fleming@yale.edu`

<sup>c</sup> *Department of Physics and Astronomy, Rutgers University*  
*Piscataway, NJ 08855, U.S.A*  
`neuberger@physics.rutgers.edu`

December 26, 2012

## Abstract

Lattice radial quantization is introduced as a nonperturbative method intended to numerically solve Euclidean conformal field theories that can be realized as fixed points of known Lagrangians. As an example, we employ a lattice shaped as a cylinder with a 2D Icosahedral cross-section to discretize dilatations in the 3D Ising model. Using this method, we obtain the preliminary estimate  $\eta = 0.034(10)$ .

---

\*Weston Visiting Scientist at The Weizmann Institute of Science.

# 1 Introduction

Conformal field theories are theoretically interesting in their own right, have applications in Condensed Matter and Statistical Physics and are relevant to Particle Physics in general. They may play a central role in the yet unknown correct description of Particle Physics beyond the Standard Model. Traditional numerical methods work well when the correlation length can be kept at a few lattice spacings but are ill suited for conformal field theories. Here we propose an untraditional numerical formulation, based on radial quantization.

A classical local Euclidean action on  $\mathbb{R}^d$  with no dimensional parameters can be rewritten in polar coordinates with radius  $r$  as a field theory on  $\mathbb{S}^{d-1} \times \mathbb{R}$  with invariance under shifts along the factor  $\mathbb{R}$  parametrized by  $\log(r)$  [1]. The shift symmetry corresponds to dilatations about the chosen origin in  $\mathbb{R}^d$ . The corresponding generator is the dilatation operator and its eigenvalues are operator dimensions. The critical new feature of our proposal is to introduce a uniform lattice discretization of  $\log(r)$ ; this provides a reasonable match between numerical resources and the relevant degrees of freedom. A lattice of linear size  $L$  in  $\log(r)$  in our proposal replaces a lattice of linear size  $e^L$  when  $\mathbb{R}^d$  is regularized directly. Using the 3D Ising model, we carry out a modest numerical test of lattice radial quantization of the Wilson-Fisher fixed point field theory.

## 2 Preserving dilatation invariance

It may sound surprising that one can regularize a field theory that is classically conformally invariant while preserving dilatations because this seems to say that an asymptotically free theory, such as QCD, does not necessarily generate a mass. We first clear up this point by studying the large  $N$  limit of the  $O(N)$  sigma model in 2D, and in the course of doing so we learn how to identify a theory that does stay conformal after quantization.

### 2.1 An example with asymptotic freedom

Consider the quantization of the two dimensional  $O(N)/O(N-1)$  nonlinear sigma model at large  $N$ , where it can be solved exactly. One can choose to preserve either dilatations together with rotations or translations in two directions, but not all of these symmetries. If one forces the preservation of all these symmetries in the quantum theory, it would end up being free. The partition function of the model is

$$Z = \int [d\phi][d\sigma] e^{-S} , \quad S = \frac{1}{2} \int d^2x [(\partial_\alpha \phi)^2 + i\sigma(\phi^2 - N/\lambda)] , \quad (1)$$

where  $\phi = (\phi_1, \phi_2, \dots, \phi_N)$  is the  $N$ -component vector field and the limit  $N \rightarrow \infty$  is taken at fixed  $\lambda$ , with  $\lambda \equiv g^2 N$ . The auxiliary field  $\sigma$  enforces the constraint  $\phi^2 \equiv \phi \cdot \phi = 1/g^2$ .

## 2.2 Standard, translation invariant analysis

At large  $N$ ,  $Z$  can be computed by saddle point. An implicit cutoff is assumed – it will be made explicit later on. In the standard approach, the global  $O(N)$  symmetry, which is nonlinearly realized at the classical level, becomes linearly realized at the quantum level by a multiplet of  $N$  massive scalar particles. Their mass,  $\mu$ , is obtained by seeking a translation invariant saddle point of the form  $\sigma(x) = -i\mu^2$ . In Fourier space we have at the saddle:

$$\phi(x) = \frac{1}{(2\pi)^2} \int d^2p e^{ipx} \tilde{\phi}(p), \quad S = \frac{1}{2} \int \frac{d^2p}{(2\pi)^2} \tilde{\phi}^*(p)(p^2 + \mu^2)\tilde{\phi}(p) - \frac{1}{2\lambda} \mu^2 N \quad (2)$$

with  $\tilde{\phi}^*(p) \equiv \tilde{\phi}(-p)$ . After integrating over the scalar fields we obtain  $Z = \int d\mu^2 e^{-NF(\mu^2, \lambda)}$ . The value of  $\mu^2$  is obtained by minimizing  $F(\mu^2, \lambda) = \frac{1}{2} \int \frac{d^2p}{(2\pi)^2} \ln(p^2 + \mu^2) - \frac{1}{2\lambda} \mu^2$  and is  $\mu = \frac{\Lambda}{\sqrt{e^{4\pi/\lambda} - 1}}$  for a UV cutoff of the form  $p^2 < \Lambda^2$ , where  $\Lambda$  is a large momentum cutoff of mass dimension. For large  $\Lambda/\mu$  we have  $\lambda \sim \frac{2\pi}{\ln(\Lambda/\mu)}$ . This is the standard result with dimensional  $\Lambda$  and  $\mu$ .

## 2.3 Dilatation invariant analysis

Following [1] we first go to radial coordinates,  $x_1 = r \cos \theta$ ,  $x_2 = r \sin \theta$  and then to Fourier space in  $\theta$ :

$$\phi(r, \theta) = \frac{1}{2\pi} \sum_{m=-\infty}^{\infty} \tilde{\phi}_m(r) e^{im\theta}, \quad \tilde{\phi}_{-m}(r) \equiv \tilde{\phi}_m^* \quad (3)$$

and

$$\sigma(x) = \frac{1}{2\pi} \sum_{m=-\infty}^{\infty} \frac{\tilde{\sigma}_m(r)}{r^2} e^{im\theta}, \quad \tilde{\sigma}_{-m}(r) \equiv \tilde{\sigma}_m^*(r). \quad (4)$$

We now map the radial coordinate to the infinite line. This step turns dilatations into translations in  $t$  and inversion into a parity in  $t$ .

$$r = e^t, \quad dr = e^t dt, \quad \Phi_m(t) \equiv \tilde{\phi}_m(r), \quad \Sigma_m(t) \equiv \tilde{\sigma}_m(r) \quad (5)$$

In the new variables the classical action is

$$\frac{1}{4\pi} \int_{-\infty}^{\infty} dt dt' \sum_{mm'} \Phi_m(t) D^{mm'}(t, t') \Phi_{m'}(t') - \frac{i}{2\lambda} N \int_{-\infty}^{\infty} dt \Sigma_0(t) \quad (6)$$

with

$$D^{mm'}(t, t') = \left[ \left( -\frac{d^2}{dt^2} + m^2 \right) \delta_{m+m', 0} + \frac{i}{2\pi} \Sigma_{-m-m'}(t) \right] \delta(t - t'). \quad (7)$$

We now look for a rotation invariant saddle point that also is translation invariant in  $t$ ,  $\Sigma_m(t) = 2\pi \bar{\Sigma} \delta_{m,0}$ . In Cartesian coordinates, such a saddle is scale invariant, but singles out one point, serving as the origin.

After integrating out the vector field, we obtain the following unregulated saddle point equation:

$$\int_{-\infty}^{\infty} dk \sum_{m=-\infty}^{\infty} \frac{1}{k^2 + m^2 + i\bar{\Sigma}} = \frac{4\pi^2}{\lambda} \quad (8)$$

The sum over  $m$  is unrestricted and can be done in closed form, producing

$$\frac{1}{4\pi} \int_{-\infty}^{\infty} dk \frac{\coth \pi \sqrt{k^2 + i\bar{\Sigma}}}{\sqrt{k^2 + i\bar{\Sigma}}} = \frac{1}{\lambda} \quad (9)$$

We now set  $i\bar{\Sigma} = \mu^2$  and choose a cutoff  $\Lambda > 0$ .  $\Lambda > 0$  is dimensionless since  $t$  was dimensionless and  $k$  is the conjugate momentum to  $t$ . We regulate by integrating over  $-\Lambda < k < \Lambda$  assuming  $\Lambda/\mu, \Lambda/\mu_0 \gg 1$ . This preserves also the  $t \rightarrow -t$  symmetry.

$$\frac{1}{4\pi} \int_{-\Lambda}^{\Lambda} dk \left[ \frac{\coth \pi \sqrt{k^2 + \mu^2}}{\sqrt{k^2 + \mu^2}} - \frac{1}{\sqrt{k^2 + \mu_0^2}} \right] = \frac{1}{\lambda} - \frac{1}{2\pi} \sinh^{-1} \frac{\Lambda}{\mu_0} \equiv \frac{1}{\lambda_R(\mu, \mu_0)} \geq 0 \quad (10)$$

$\lambda_R$  is a renormalized coupling.  $\mu$  and  $\mu_0$  are dimensionless.  $\mu_0$  is an arbitrary renormalization point. The bare coupling depends on the cutoff in the standard way, except the cutoff is dimensionless:  $\lambda \sim \frac{2\pi}{\ln(2\Lambda/\mu_0)}$ . A nonzero saddle point will always be found. The saddle point value  $\mu$  never exceeds a maximal value, which depends on  $\mu_0$  and is defined by

$$\mu_{\max}(\mu_0) : \int_{-\infty}^{\infty} dk \left[ \frac{\coth \pi \sqrt{k^2 + \mu_{\max}^2(\mu_0)}}{\sqrt{k^2 + \mu_{\max}^2(\mu_0)}} - \frac{1}{\sqrt{k^2 + \mu_0^2}} \right] = 0. \quad (11)$$

The propagator of the scalar field is

$$\langle \Phi_{m'}^{*i}(t) \Phi_m^j(t') \rangle = \delta^{ij} \delta_{mm'} \int_{-\infty}^{\infty} \frac{dk}{2\pi} \frac{e^{ik(t-t')}}{k^2 + m^2 + \mu^2} = \delta_{ij} \delta^{mm'} \frac{e^{-\sqrt{m^2 + \mu^2}|t-t'|}}{2\sqrt{m^2 + \mu^2}}. \quad (12)$$

## 2.4 Cartesian Translation Invariance

Reading off the set of dilatation eigenvalues displayed by eq. (12) we see that it does not contain an equally spaced ladder. Consequently, we cannot construct translation generators satisfying the correct commutation relations [2] with dilatations in the sector generated by the action of  $\Phi$  on the vacuum. The deviation of the dilatation spectrum from equal spacing is small if  $m \gg \mu$ . There is approximate translation invariance for angular separations that are small relatively to  $\frac{1}{\mu}$ . Such separations can be resolved only by waves with high enough angular momenta  $m$ . Because inversion has also been preserved in the quantization, if translations could be realized, special conformal transformations would come in automatically and the full conformal group would be realized. Because of rotation invariance, only one linear combination of translations needs to be considered in detail.

Comparing the manipulations we did here to those we would have done had we declared we are interested in the traditional view of the model at finite non-zero temperature, we realize that while the language has changed, the equations have not. There exists only one bosonic vector  $O(N)/O(N-1)$  sigma model on  $\mathbb{S} \times \mathbb{R}$ . In traditional terms, the circumference of  $\mathbb{S}$  in units of the dynamically generated mass at zero temperature is a free parameter. Insisting that  $\mathbb{S}$  is a geometric circle made its length equal to  $2\pi$  in the untraditional view. In traditional terms the propagator decays exponentially in the Cartesian spacetime directions, while in untraditional terms the propagator decays exponentially in the coordinate conjugate to the dilatation generator.

## 2.5 One useful lesson

We did not get anything truly new in the untraditional quantization; the “novelty” boiled down to semantics. But, we learned a lesson which will be useful in the following: if we started from a classical conformal theory that allowed this symmetry to be fully preserved at the quantum level and chose to preserve dilatations and rotations explicitly by the cutoff procedure, translations would be restored in the continuum limit. The generators of translations could be reconstructed from the commutation relations of the conformal algebra using the available generators of rotations, dilatation and inversion [2]. Eventually we would get the same theory we would have gotten from a traditional lattice regularization that preserved a discrete version of translations from the start but left dilatations and rotations unpreserved. However, at the lattice regulated level, the choice to preserve dilatations seems more efficient.

## 3 Lattice radial quantization in three dimensions

In the continuum we would be dealing with a theory on  $\mathbb{S}^2 \times \mathbb{R}$ . The critical exponents of the same CFT on  $\mathbb{R}^3$  can be extracted from the dilatation operator on  $\mathbb{S}^2 \times \mathbb{R}$  [3]. In the two dimensional case one has  $\mathbb{S} \times \mathbb{R}$  and the same can be done [4]. This works well because the factor  $\mathbb{S}$  is easy to discretize. In three dimensions we need to discretize  $\mathbb{S}^2$  and it becomes impossible to replace the continuum  $O(3)$  symmetry by symmetries under ever larger discrete subgroups as the lattice is refined. One is limited to a few discrete subgroups. Hopefully, this gets compensated by their stronger, nonabelian structure. One can latticize  $\mathbb{S}^2$  [3] by the set of vertices of a platonic solid, but this does not work well [5]. A way to improve on this is to use regular lattice refinements of the faces of the platonic solid [6]. For a cube, this approach produced reasonably accurate exponents in the  $Z_2$  even sector of the Ising model. However, the estimate of the exponent  $\eta$  in the odd sector had a substantially larger deviation from the known value [7]. Our numerical experiment will exploit the lesson we learned in the previous section on a lattice similar to that of [6].

To have as much symmetry as possible we employ a closed two dimensional surface

$\Sigma$ , consisting of the boundary of an icosahedral solid instead of a cube. The linear distances between points on  $\Sigma$  and the origin are bounded to a relatively narrow interval on the positive axis. The icosahedron has 12 vertices and 20 faces given by identical flat equilateral triangles. Its symmetry group  $I_h$  is a 120 element subgroup of  $O(3)$ . The angular momenta  $l = 0, 1, 2$  representations of  $O(3)$  remain irreducible representations under  $I_h$ . This is enough to isolate a scalar primary state and two of its immediate descendant states on the basis of their behavior under  $I_h$ .  $\mathbb{R}^3$  is visualized as a set of 20 infinite triangular pyramids glued together with the apexes meeting at the origin. In isolation, each pyramid can be (non-conformally) mapped into a uniform prism with an equilateral triangle as cross section. These prisms are then glued together in a manner inherited from the pyramids. We end up with  $\Sigma \times \mathbb{R}$ .

We regularize  $\Sigma$  by replacing each face by a triangular piece of a regular two dimensional triangular lattice. Consequently, each side of the original triangle has extra  $s - 1$  equally spaced points placed on it ( $s \geq 1$ ). The number of sites on one icosahedral shell is  $2 + 10s^2$ . Identical grids replacing  $\Sigma$  are strung along an equally spaced infinite straight line, making up a cylinder. Matching vertices on neighboring  $\Sigma$ -slices are connected by links of equal lengths.

For a finite cylinder, the partition function is of the usual form,

$$Z = Tr_{\sigma} e^{\sum_{t,i} \beta \sigma(t,i) \sigma(t+1,i) + \sum_{t,\langle ij \rangle} \beta \sigma(t,i) \sigma(t,j)}, \quad (13)$$

where  $\langle ij \rangle$  denotes a nearest-neighbor pair on the same icosahedral shell and  $t = 0, \dots, T - 1$  labels the shells along the cylinder. The trace is a sum over the Ising spin values  $\sigma(t,i) = \pm 1$  for all sites  $(t,i)$ .

To get to the continuum limit of the Wilson-Fisher conformal field theory, we need to tune  $\beta$  to its infinite  $s$  critical point. The coupling  $\beta$  has been chosen the same in all directions for simplicity. The intra-shell lattice spacing and the lattice spacing on the triangulated shells are fixed by demanding that descendants have equal unit spacing as we approach the continuum limit. This is a self-consistent definition only if the descendant ‘‘masses’’ fall on a straight line. This happens only at the critical value of  $\beta$ . To get information on the spectrum of the transfer matrix it is convenient to compactify the infinite axis of the cylinder to a circle with periodic boundary conditions on the spins. We chose our cylinders to have lengths  $T$  which scale with the refinement as  $T = \rho s$ .

Our focus is on the 3D Ising critical exponent  $\eta$ . This number is determined by the dimension  $\Delta_{\sigma}$  of the lowest primary in the  $Z_2$  odd sector of the space the transfer matrix acts on. To get the primary state and some of its descendants we define field variables on each  $t$ -labeled shell:

$$\tilde{\sigma}(t, l, m) = \sum_i \Delta \Omega_i Y_l^m(\theta_i, \phi_i) \sigma(t, \theta_i, \phi_i). \quad (14)$$

$\Sigma$  is parameterized by the polar and azimuthal angles  $\theta, \phi$ .  $t$  corresponds to the logarithm of the amount of dilatation a specific  $\Sigma$  embedded in  $\mathbb{R}^3$  would have undergone. The  $Y_l^m(\theta, \phi)$  are the standard spherical harmonics with  $l = 0, 1, 2$ . The measure  $\Delta \Omega_i$  is computed from the area of the spherical triangles adjacent to  $\theta_i, \phi_i$  projecting onto a unit sphere in order to assure a

rapid convergence to the orthonormality condition for the  $Y_l^m(\theta, \phi)$ 's in the continuum. The  $I_h$  symmetries and dilatations guarantee  $\langle \tilde{\sigma}(t, l, m) \tilde{\sigma}(t', l', m') \rangle = C_l(t - t') \delta_{ll'} \delta_{mm'}$  for  $l, l' = 0, 1, 2$  with  $|m| \leq l$ ,  $|m'| \leq l'$ . From the  $l = 0$  channel we get the dimension of the primary state and from the  $l = 1, 2$ -channels the dimensions of the next two descendant states. We denote these three eigenvalues of the dilatation operator by  $\Delta_l$ , where  $\Delta_l$  plays the role of a mass when  $t$  is regarded as a time variable. The eigenvalues of the lattice dilatation operator corresponding to the continuum dimensionless numbers  $\Delta_l$  are denoted by  $\mu_l$ . The theory now has an ultraviolet cutoff denoted by  $\Lambda$ .  $\Lambda^{-1}$  is dimensionless, determining the smallest angular separation on the discretized  $\Sigma$ .

$$\Delta_l = \mu_l \Lambda \quad (15)$$

$\Lambda \propto s$  as  $s \rightarrow \infty$  and we anticipate an integer spacing of descendants,  $\Delta_l = \Delta_0 + l$ , in the  $s \rightarrow \infty$  limit. Having three values of  $\mu_l$  at our disposal due to the icosahedral symmetry, we can test numerically whether they indeed fall on one straight line. The slope of this line determines  $\Lambda$  and fixes the ratio of the lattice spacing on the sphere relative to radial axis in  $t$ . The  $\mu_l$  will go as  $s^{-1}$  at large  $s$  and the standard critical exponent  $\eta$  is given by the anomalous portion of  $\Delta_l$  for any  $l$ :  $\eta = 2(\Delta_l - l - 1/2)$ .

It is known that  $\eta$  is small relative to 1 [7]. This puts a high accuracy demand on the  $\mu_l$ 's, which are the directly measurable quantities.

## 4 Results

First the critical point  $\beta_c$  was determined by computing the 4th-order Binder cumulant [8],

$$U(\beta, s, \rho) = 1 - \frac{\langle M^4 \rangle}{3 \langle M^2 \rangle^2} . \quad (16)$$

Our initial computations of moments of the magnetization were performed using the Swendsen-Wang cluster algorithm [9]. Later, we switched to the more efficient [10] single cluster Wolff algorithm [11]. To locate the critical point, we used aspect ratios  $\rho = 4, 8$ . with  $s \geq 16$  and  $\beta$  such that  $|\beta - \beta_c| s^{1/\nu} \leq 0.0012$ . We then fit the data to:

$$U(\beta, s, \rho) \simeq U(\beta_c, \infty, \rho) + a_1(\rho) [\beta - \beta_c] s^{1/\nu} + b_1(\rho) s^{-\omega} . \quad (17)$$

Subsets of the data used appear in Fig. 1. The best fit gave  $\beta_c = 0.16098691(1)$  with critical Binder cumulants  $U(\beta_c, \infty, 4) = 0.3032(1)$  and  $U(\beta_c, \infty, 8) = 0.18765(5)$  with a  $\chi^2/\text{dof} = 1.37$ ,  $\text{dof} = 212$ . The best-fit exponents  $\nu = 0.621(4)$  and  $\omega = 0.797(6)$  are consistent with the values in [7] at the 2-sigma level.

To compute the correlation functions,  $C_l(t) = \langle \tilde{\sigma}(t + t_0, l, m) \tilde{\sigma}(t_0, l, m) \rangle$ , we generated ensembles at  $\beta = 0.160987$ . Our final results for  $\beta_c$  from the Binder cumulant suggest this might be slightly in the ordered phase as  $s \rightarrow \infty$ . Each independent run was thermalized using 2048 sweeps of the Wolff algorithm followed by 8192 sweeps with one estimate of the correlation

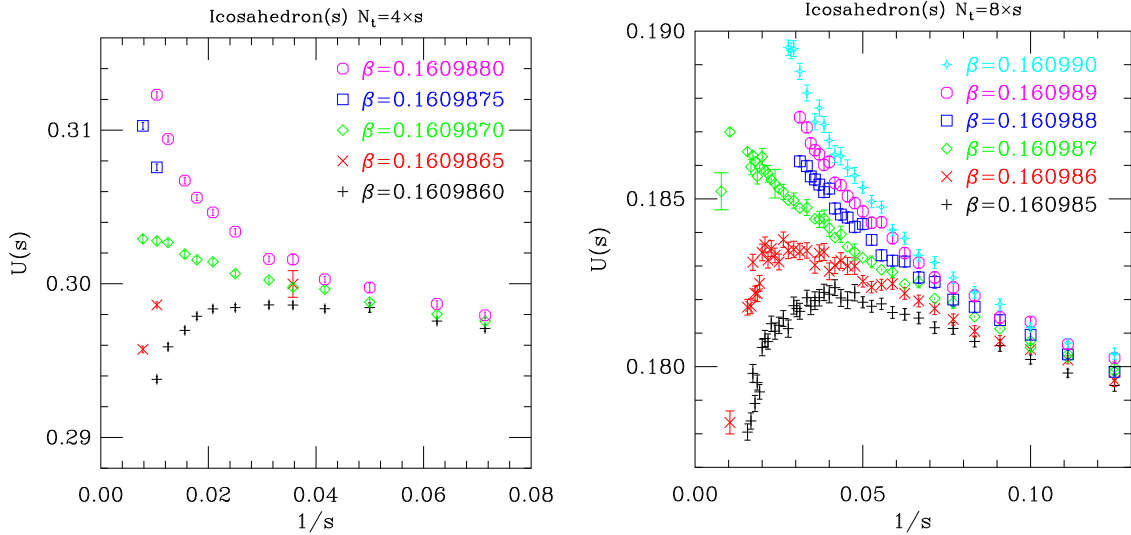


Figure 1: Determining  $\beta_c$  from the Binder cumulants  $U(s) = 1 - \langle M^4 \rangle / 3 \langle M^2 \rangle^2$  near the pseudo-critical point for two different aspect ratios  $\rho$  and increasing values of  $s$ .

function after each sweep. We defined a sweep to be  $19s/2$  Wolff cluster updates. This choice sets the average number of spins flipped per sweep to be about equal to the total volume. All results for a given run are then averaged together to form a single blocked estimate and many thousands of independent block estimates are combined to form the ensemble at each  $s$ , as shown in Table 1. The jackknife method was used to estimate errors.

$s$	8	9	10	11	12	14	16	18	20	22	24
$N$	19456	19999	20480	20000	18975	20480	23552	22528	19328	10624	10202
$s$	28	32	36	40	44	48	52	56	58	64	
$N$	6656	25792	8832	15168	13608	2528	7935	8017	1088	1000	

Table 1:  $N$  is the number of independent runs used for the correlation function at each refinement  $s$ . Other details of the runs are described in the text.

We found it very useful to evaluate the correlation function using the momentum-space single cluster improved estimator method [12, 13]. As we are only interested in the rotation-invariant part of the correlation function on any given lattice, we also average over the  $m = -l, \dots, l$  states in the various representations labeled by  $l$ . Since our value of  $\beta$  should be slightly larger than the pseudo-critical coupling at any finite  $s$ , we expect that our  $l = 0$  correlation function will have a small disconnected contribution, which should vanish as  $s \rightarrow \infty$ , assuming  $\beta = \beta_c$ . If the disconnected contribution remained non-zero, it would suggest that  $\beta > \beta_c$ ; otherwise, we would conclude that  $\beta < \beta_c$ . The contribution of the lowest eigenstate of the transfer matrix to the connected correlation function in momentum space is given by

$$\tilde{C}_l(k) = c_0 \delta_{l,0} \delta_{k,0} + a_l \frac{(1 - e^{-\mu_l T}) \sinh(\mu_l)}{\sinh^2(\mu_l/2) + \sin^2(k/2)}, \quad (18)$$



where  $k = 2\pi n/T$  with  $n = 0, \dots, T-1$  is the momentum conjugate to  $t$  along the cylinder and we have included the disconnected contribution  $c_0$ . We can determine  $c_0$  by fitting  $\tilde{C}_0(k)$  for  $k \neq 0$  and subtracting a smooth extrapolation of  $\lim_{k \rightarrow 0} \tilde{C}_0(k)$ . We found that our data required parameterizing the lowest eigenvalue plus at least two higher eigenvalues. We got excellent fits with  $\chi^2/\text{dof} \lesssim 1$  and estimates of the lowest eigenvalues which are essentially free of contamination. The result is shown in Fig. 2. A linear extrapolation in  $1/s$  indicates that the disconnected contribution vanishes at finite  $s \approx 64$ . Then,  $\beta = 0.160987 < \beta_c$ , in apparent contradiction to the Binder cumulant result.

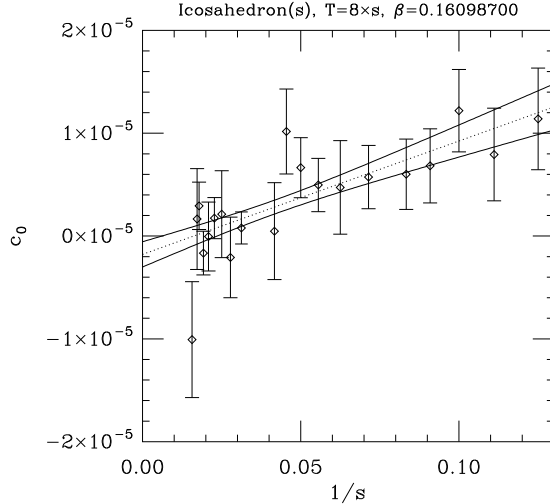


Figure 2: The disconnected contribution to the correlation function as described in the text.

We relate the  $\mu_l$ 's for  $l = 0, 1, 2$  to the eigenvalues of the dilatation operator by  $\mu_l = \Lambda^{-1}[\Delta_0 + l]$  where  $\Lambda^{-1} \simeq c_1/s$  as  $s \rightarrow \infty$ . We find  $c_1 \approx 1.51(1)$  with the uncertainty dominated by systematic error. The left figure of Fig. 3 shows evidence for also sub-leading contributions,  $\mathcal{O}(1/s^2)$ . We confirm the equal spacing rule of descendants by examining the ratios,  $(\mu_{l+2} - \mu_{l+1})/(\mu_{l+1} - \mu_l)$ , as shown on the right in Fig. 3. We are now justified to estimate the scaling dimension of the primary operator using

$$\Delta_0 = \frac{l - l'}{2} \left[ \frac{\mu_l + \mu_{l'}}{\mu_l - \mu_{l'}} - \frac{l + l'}{l - l'} \right] \quad (19)$$

as shown in Fig. 4. The determination is independent of  $\Lambda$ .

A quite conservative estimate is  $\eta = 0.034(10)$ , consistent with other estimates [7]. Our numerical study could be extended to include additional primary operators in both the  $Z_2$ -odd and  $Z_2$ -even sectors as well as a direct test of the restoration of full conformal symmetry for 2- and 3-point correlators. However as a cautionary note, we now briefly describe the behavior of the eigenvalues for the descendants with  $l = 3$ .

The 7-dimensional  $l = 3$  irrep of  $O(3)$  splits under  $I_h$  into the sum of the 4-dimensional irrep  $G$  and the 3-dimensional irrep  $T_2$ . The  $l = 3$  states  $m = \pm 2, \pm 3$  appear in both irreps of

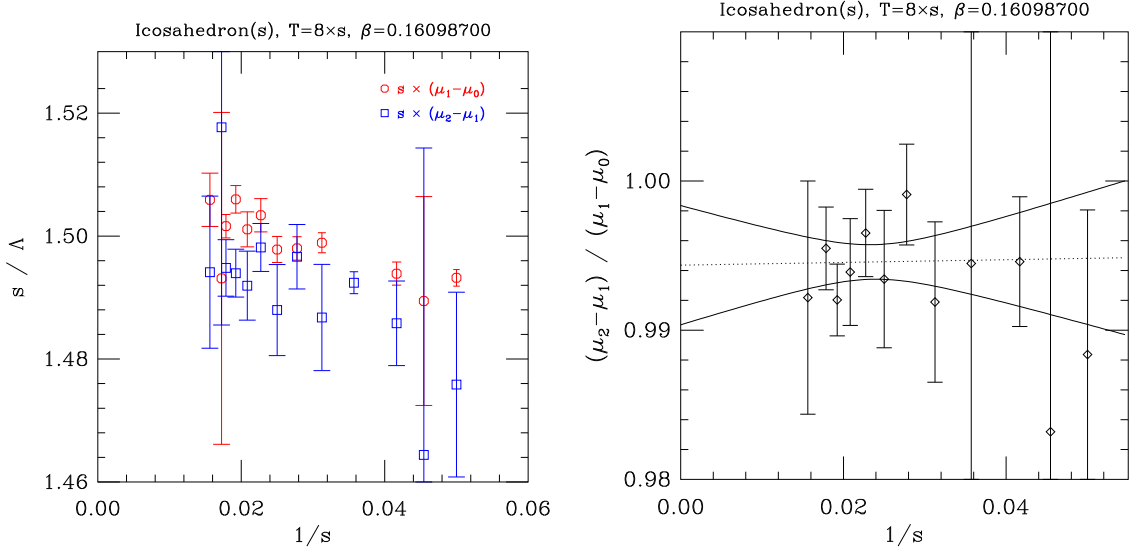


Figure 3: The left figure shows the scaling of  $\Lambda$  with  $s$ . The extrapolated value is 1.51(1) with the uncertainty dominated by the systematic difference between the two estimates. The right figure checks whether the  $\mu_l$  fall on a straight line. We fit to a linear function and find an intercept of 0.994(4) and slope of 0.0(2) with  $\chi^2/\text{dof} = 0.43$  for 11 dof.

$I_h$  but the states  $m = \pm 1$  only appear in  $G$ , while the state  $m = 0$  only appears in  $T_2$ . In Fig. 5 we show the  $l = 3$  eigenvalues labeled by  $m = 0, \pm 1$ . If they extrapolated to the same value as  $s \rightarrow \infty$ , it would be an indication that  $O(3)$  symmetry is restored in the continuum limit. The numerical evidence so far suggests the contrary, indicating that the continuum limit with the icosahedral shell is not fully reproducing the conformal fixed Wilson-Fisher fixed point of the 3D Ising model on flat three-space. More refined methods are needed, as suggested below.

## 5 Discussion and Outlook

The method of lattice radial quantization presented in this paper holds promise as a practical nonperturbative tool for conformal field theory. We plan additional numerical and theoretical studies to realize this goal.

An important theoretical question remains: How do exponents associated with  $l = 0, 1, 2$  in our icosahedral shell system at  $s \rightarrow \infty$  relate in principle to their exact  $\mathbb{R}^3$  values in the 3D Ising model? The numbers in [6] and our  $\eta$ -value are consistent with equality, but are far from providing overwhelming numerical evidence. Indeed, the apparent lack of convergence to a single  $O(3)$  irreducible representation for  $l = 3$  in Fig. 5 suggests that the continuum limit of our radial-icosahedral model is not equivalent to the 3D Ising model at the Wilson-Fisher fixed point on flat three space. A failure to reproduce the correct spectral degeneracy of  $l > 2$  descendants

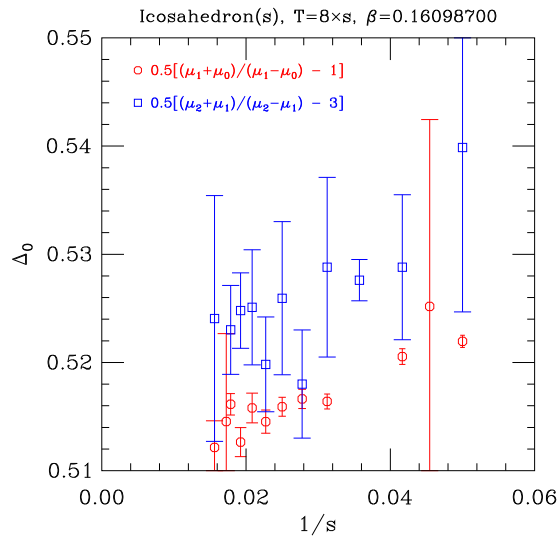


Figure 4: The scaling exponent of lowest  $Z_2$ -odd primary operator *vs.*  $1/s$ . The lower (red) points come from  $\mu_0$  and  $\mu_1$ . The determination of  $\mu_0$  is unreliable because of the disconnected contribution to the correlator, given the uncertainty whether  $\beta_c < 0.160987$   $\beta_c > 0.160987$ . A linear extrapolation from upper (blue) points, based on  $\mu_1$  and  $\mu_2$ , gives  $\Delta_0 = 0.517(5)$ , which is consistent with the estimate  $0.5182(3)$  in [7].

at  $s \rightarrow \infty$  would indicate distorted spectra for the primaries as well. The icosahedral shell may be sufficiently spherical to keep these distortions in  $\eta$  to a level below our current estimate.

We are now studying in the continuum the consequence of quantization on  $\Sigma \times \mathbb{R}$  where  $\Sigma$  is sectionally flat. Also, we are implementing improved actions for our lattice representation with nearest neighbor bonds weighted to approach the continuum metric on  $\mathbb{S}^2 \times \mathbb{R}$ , similar to the discretization employed for our single spin operators. Both theoretical considerations and numerical tests are needed to clarify how a radial lattice can reproduce a conformal Euclidean field theory on flat space in the continuum limit.

Lattice radial quantization should apply also to four dimensional gauge theories with an amount of matter where the IR behavior is suspected to be controlled by an interacting conformal theory. Historically, interest in such theories was motivated by a search for realizations of walking Technicolor scenarios [14] in their vicinity. Independently of the relevance of the latter to Nature, there is theoretical interest in these theories, in particular in the large  $N$  limit for the gauge group  $SU(N)$  because of the potential existence of a specific string dual in the IR. In the case of 4D gauge theories, the anomalous dimensions of interest are typically large, so the demands on numerical accuracy are weaker than those for  $\eta$ .

**Acknowledgments:** RCB acknowledges support under DOE grants DE-FG02-91ER40676, DE-FC02-06ER41440 and NSF grants OCI-0749317, OCI-0749202. RCB has benefited from

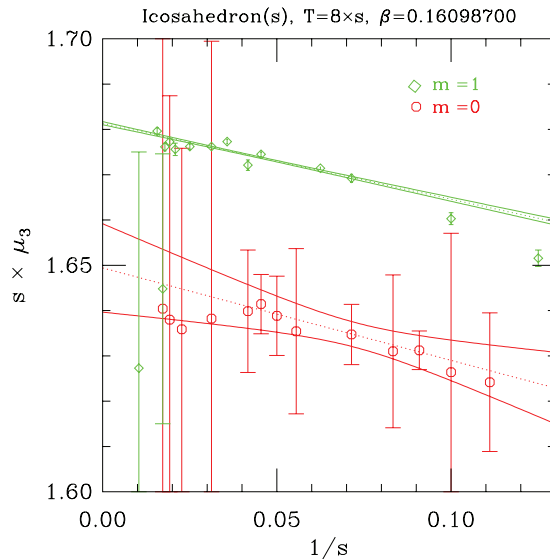


Figure 5: The eigenvalues  $\mu_3$  for the  $l = 3, m = 0, \pm 1$  descendants of the lowest  $Z_2$ -odd operator *vs.*  $1/s$ . The lower (red) circles are  $m = 0$  and the upper (green) diamonds are  $m = \pm 1$ . The difference is a measure of the breaking of  $O(3)$  symmetry at that  $s$ .

conversations with Joseph Minahan. GTF acknowledges partial support by the NSF under grant NSF PHY-1100905. RCB and GTF also thank the Galileo Galilei Institute for Theoretical Physics for the hospitality and INFN for partial support during the workshop “New Frontiers in Lattice Gauge Theories”. HN acknowledges partial support by the DOE under grant number DE-FG02-01ER41165. HN is grateful for support under the Weston visiting scientist program at the Weizmann Institute in the Faculty of Physics. HN has benefited from conversations with Micha Berkooz, Rajamani Narayanan and Adam Schwimmer.

## References

- [1] S. Fubini, A. J. Hanson and R. Jackiw, Phys. Rev. D **7**, 1732 (1973).
- [2] Efim S. Fradkin and Mark Ya. Palchik, “Conformal Quantum Field Theory in  $D$ -dimensions”, Kluwer Academic Publisher, 1996.
- [3] J. L. Cardy, J. Phys. A **18**, L757 (1985).
- [4] J. L. Cardy, J. Phys. A **17**, L385 (1984).
- [5] F. C. Alcaraz and H. J. Herrmann, J. Phys. A **20**, 5735 (1987).
- [6] M. Weigel and W. Janke, Physica A **281**, 287 (2000).
- [7] A. Pelissetto and E. Vicari, Phys. Rept. **368**, 549 (2002) [cond-mat/0012164].

- [8] K. Binder, Z. Phys. B **43**, 119 (1981).
- [9] R. H. Swendsen and J. -S. Wang, Phys. Rev. Lett. **58**, 86 (1987).
- [10] P. Tamayo, R. C. Brower and W. Klein, J. Statist. Phys. **58**, 1083 (1990).
- [11] U. Wolff, Phys. Rev. Lett. **62**, 361 (1989).
- [12] C. Ruge, S. Dunkelmann, F. Wagner and J. Wulf, J. Statist. Phys. **73**, 293 (1993).
- [13] C. Ruge, P. Zhu and F. Wagner, Physica A **209**, 431 (1994) [hep-lat/9403009].
- [14] T. W. Appelquist, D. Karabali and L. C. R. Wijewardhana, Phys. Rev. Lett. **57**, 957 (1986).